

Chinese karst geology and measures to prevent geohazards during shield tunnelling in karst region with caves

Qing-Long Cui · Huai-Na Wu · Shui-Long Shen · Ye-Shuang Xu · Guan-Lin Ye

Received: 3 November 2014 / Accepted: 30 December 2014 / Published online: 8 January 2015
© Springer Science+Business Media Dordrecht 2015

Abstract Karst landscapes are widely distributed in China, and buried karst is widespread in Guangdong. This study mainly focuses on buried karst or karst caves which are underground at depths of up to 50 m and can significantly affect engineering construction activity. The karst caves, which are widely distributed in Guangdong Province, have the following features: high fissure water content, high rock permeability, prone to collapse, variable shapes, and irregular distribution. When a shield tunnel is constructed in this kind of environment, hazards, such as sink holes, the ingress of water or stones, and damage to the constructed tunnels may occur. Thus, karst caves need to be treated before tunnel construction. This paper presents a procedure for karst cave treatment to mitigate possible hazards during shield tunnelling in karst regions. The construction procedure includes field investigation, judgment, treatment, and effectiveness check. The treatment criteria, grouting material, construction steps, and effectiveness check for the karst cave treatment are introduced in detail. A field test on shield tunnelling excavation was conducted using the karst cave treatment in the karst region of Guangzhou, China. Field investigations include testing the unconfined compressive strength (UCS) of borehole samples of grouting materials, standard penetration test (SPT), core recovery (CR), ground surface settlement and building settlement. All of the UCS values of the borehole samples are greater than 0.2 MPa, the modified SPT values are more than ten, and the CR values are greater than

Q.-L. Cui · H.-N. Wu · S.-L. Shen (✉) · Y.-S. Xu · G.-L. Ye
State Key Laboratory of Ocean Engineering, Department of Civil Engineering, Shanghai Jiao Tong University, Shanghai 200240, China
e-mail: slshen@sjtu.edu.cn

Q.-L. Cui
e-mail: cq1@sjtu.edu.cn

H.-N. Wu
e-mail: wu-hn@sjtu.edu.cn

Y.-S. Xu
e-mail: xuyeshuang@sjtu.edu.cn

G.-L. Ye
e-mail: ygl@sjtu.edu.cn

90 %. The measured values of ground surface settlement and building settlement are all within the allowable ranges. All of the test results demonstrate the applicability of this treatment process in karst regions.

Keywords Tunnelling in karst · Hazards · Karst cave treatment · Field trial · Settlement

1 Introduction

With the rapid urbanization in China during the last three decades, large numbers of underground structures have been constructed, of which metro and railway tunnels account for the largest proportion (Liao et al. 2008, 2009; Tan and Wang 2013a, b; Shen et al. 2006, 2009, 2010, 2014; Xu et al. 2008, 2012a, b; Wu et al. 2014). There are 41 cities with metro tunnels in operation or under construction, including Beijing, Shanghai, Guangzhou, and Shenzhen. During construction of metro tunnels, the following three types of strata are often encountered: soft soils (clay, silt, and sand) (Xu et al. 2013a, b; Ma et al. 2014), sand and gravels, and mixed ground (karst, variably weathered granite) (Shin et al. 2006; Zhao et al. 2007; Standing and Selemetas 2013; Tóth et al. 2013; Fagnoli et al. 2013). Although there are many reports on tunnelling in soft soils and sand and gravels, tunnel excavation in karst regions is not discussed in the existing literature (Zhang et al. 1993; Yang et al. 2007; Gui 2008; Ju and Zhu 2007; Li et al. 2013; Li and Li 2014; Shen and Xu 2011; Shen et al. 2013a, b, c).

Every karst cave starts with microkarst corrosion, and then, a cave system is developed through a long process. Karst is widely distributed in China. Indeed, there are seven primary karst areas in China. Each area has its own characteristics, and there are many karst types, such as subterranean river-type caves, sink hole-type caves, through caves, phreatic caves along river valleys, vadose caves, and tufa caves. In southern China, there is buried karst, which has high fissure water content, is prone to collapse, has high permeability, is of variable shapes, and is irregularly distributed. Guangzhou, a metropolis also in southern China, has an extensive metro tunnel system. As of the end of December 2013, there were 9 lines and 164 stations in operation, with a total length of about 260.5 km. By 2020, the metro system will expand to 17 lines totalling 677 km in length according to the Guangzhou Urban Rapid Rail Transit plan. The tunnel construction methods include the shield method, the mining method, and the cut and cover method, of which the shield method is the most frequently used in the city. Shallow-buried tunnels that range from 10 to 30 m in depth are often adopted in the design and construction of the Guangzhou metro.

However, the karst cave environment exerts a significant impact on shield tunnel excavations. During tunnel construction using the shield method in the karst cave stratum, karst caves can cause a number of hazards, such as sink holes, water or stone ingress, damage to constructed tunnels and the shield machinery, and long-term instability. To ensure construction safety and the successful advance of the shield, and to provide adequate bearing capacity for the operating metro line, a karst cave treatment is proposed taking into account the properties of the surrounding soil and rock and whether the karst caves are already filled with debris.

The objectives of this paper are as follows: (1) to investigate the distribution of karst in China; (2) to discuss potential geohazards during tunnelling in karst caves; (3) to introduce

the karst cave treatment; and (4) to verify the effect of the treatment process through a case study.

2 Karst geology in China

2.1 Distribution of karst in China

Karst topography is a landscape formed from the dissolution of soluble bedrocks, which are usually carbonate rock (e.g. limestone, dolomite), sulphuric rock (e.g. gypsum, mirabilite), and halogenated rock (rock salt) (Lu 2010). It is widely distributed throughout China. In the vast karst areas of China, different characteristics are displayed in different regions due to the effect of various natural environmental factors. In general, there are two kinds of karst: (1) pure karst, which is carbonatite karst, and (2) composite karst, which includes sulphates and halides. The formation of a karst system (Yuan 1976), which can be hundreds of kilometres in length, is a long process that starts with microkarst corrosion. Initially, erosion leads to the formation of voids with a diameter of 0.1–5 cm. Then, when the erosion continues and the void is extended in particular areas, it gradually develops into channels of several kinds. If these channels subsequently become connected, then a karst system is created.

According to the geological structure and the climatic conditions, the karst in China is divided into seven zones. Figure 1 shows a karst zoning map of China. The characteristics of each karst area are as follows:

- a. Tibetan Plateau karst area (A): the Tibetan Plateau area consists of the Himalayas and the Tibetan Plateau at an altitude above 3,500 m. The area of large basins on Tibetan Plateau can be 11,500–51,300 km². This area has many carbonate rocks from the Palaeozoic to the Cenozoic eras. There is also sulphuric rock and halogenated rock in salt lakes in the Tibetan Plateau. Since the Mesozoic era, the crustal movement has

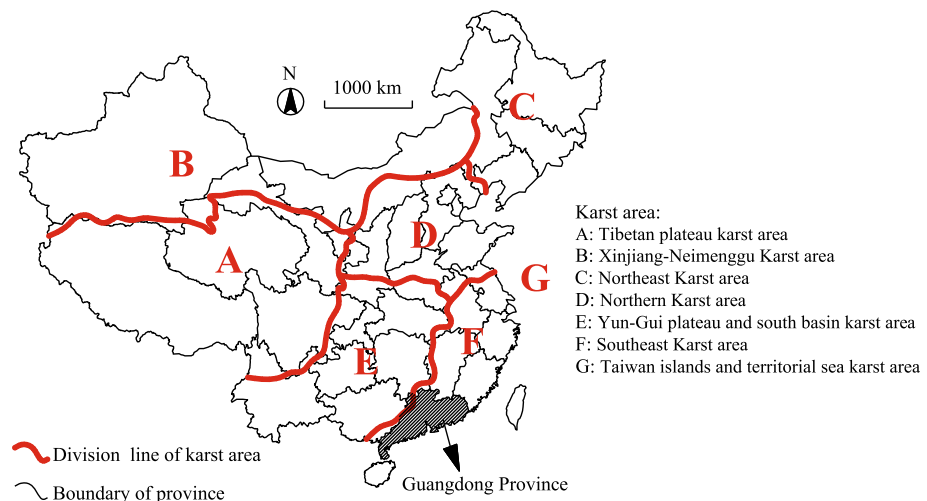


Fig. 1 Karst zoning map of China (created based on CK2010)

- thrown up the Himalayas and the Tibetan Plateau, resulting in a very cold, arid, and semi-arid climate. Karst in this area is formed mainly due to glacial erosion and denudation. The maximum flow of karst springs on Tibetan Plateau is $2 \text{ m}^3/\text{s}$.
- b. Xinjiang-Neimenggu karst area (B): carbonate rocks are mainly exposed in the Sinian, Cambrian, and Ordovician periods. At the height of 4,400–5,600 m, there are many forms of karst, including stone forest and karst mountains. For example, the altitude of Kuikewusu stone forest is 3,500 m, the length is 9 km, and the width is 5 km. Karst is highly developed in mountainous areas due to water erosion and glacial erosion of the carbonate rocks. Under the Tarim Basin, there also exists buried karst, at depths of more than 5,000 m. There is deep-buried karst under Taklimakan Desert (at the depth of tens of 1,000 m). As the content of potassium salt in Luobu Lake of Xinjiang is huge, there exist many forms of karst, for example, salt crust with solution crack.
 - c. North-east karst area (C): the average rainfall in this area is 300–700 mm. The thickness of carbonatite can be 5,000 m. The elevations of many mountains are over 1,000 m. In Yichun of Heilongjiang Province, karst develops and karst sink holes are distributed here. The thickness of rock stratum is 292–1,773 m. At underground river of Benxi of Liaoning Province, the width of water is 13.15 m, the depth of hole is 3,000 m, and the flow can be $14,428 \text{ m}^3/\text{day}$. In the Liaotung Peninsula, there is seashore karst and seabed karst. Carbonatite underground rivers and karst springs are also widely distributed. And their flows rate can be $0.5\text{--}1.25 \text{ m}^3/\text{day}$. Mountain karst caves and large karst springs are found in the Xiao Hinggan Mountains in the north of Heilongjiang Province. The movement of volcano hydrothermal karst results in mineral resources in this area.
 - d. Northern karst area (D): the maximum thickness of carbonatite can be 11,000 m, and the average thickness is 3,000–5,000 m. This area includes the Taihang Mountains, the Shanxi Plateau, Yanshan in Beijing, and Nanshan in central Shandong. Karst here mainly consists of naked and half-naked karst, karst exposed by corrosion and by tectonic processes. Buried karst is also widely distributed here. There are many karst springs, which serve as an important water source for the Taihang Mountains, the Shanxi Plateau, and Nanshan District in Shandong. During coal mining, the inrush of karst water often causes danger. The maximum inflow rate of water is $7.38 \text{ m}^3/\text{day}$, and water bursting discharge is $0.8\text{--}4 \text{ m}^3/\text{day}$.
 - e. Yun-Gui Plateau and south basin karst area (E): the carbonate rock karst in this area is most densely distributed and exists in many types. Extensive karst landforms are found, including soluble depressions, peak forest valleys, isolated peak plains, and subsurface streams. The Fairy Cave in Guizhou Province is a reticular cave system which comprises 12 connected caves. Carbonatite is distributed in 75 % area of Dushan of Guizhou, and its height is 1,200–1,300 m. Canyon karst is located in the east of Chongqing City. Sichuan Basin is eroded by the Three Gorges Dam System. Many karst mountains are located in Guangxi and Guilin provinces.
 - f. South-east karst area (F): carbonate rocks are widely but not continuously distributed in this area due to the cutting effect of tectonic movement and the intrusion of igneous rocks. The average thickness of carbonate rocks in this area is 1,000–4,500 m. The landform in this area is mainly hills formed by water erosion. Due to the intrusion of igneous rock, erosion of karst results in metallic mineral resources like iron. Karst lakes exist extensively in Tai Lake and West Lake. Mountain karst caves and large karst springs are found in Yangtze River Delta and the Pearl River Delta. There is much buried karst in Guangdong Province, and it will be introduced in details in the following.

- g. Taiwan Islands and territorial sea karst area (G): in this area, carbonate rocks have grown into a stone forest landscape, and coral reefs have transformed into eroded cliffs, cavities, and pillars. Karst in and around Taiwan is mainly medium–high mountain gorge-type karst and coral reef karst. The coral reef karst in South China Sea and Hainan Island mainly comprises of over 300 kinds of coral polyps. The growth speed of coral polyps varies with areas. For example, the growth speed of fungus is 4–5 mm/a in South China Sea and 12 mm/a in Hainan Island.

2.2 Buried karst with caves in Guangdong Province

The karstification of a landscape may result in a variety of features both on the surface and underneath the ground. Based on the exposure conditions, the karst is classified into two categories: (1) exposed and semi-exposed karst, and (2) buried karst.

Buried karst is widely distributed in Guangdong Province, which is in the south-east karst area (F). One kind of buried karst exists below the quaternary soil strata. Some of the buried karst had once been exposed karst on the ground, and was then covered. Karst erosion is still ongoing. According to the depth of the quaternary soil strata, that found at a depth of less than 100 m is shallow-buried karst, and that found at a depth of more than 100 m is deep-buried karst (Lu 2010). Buried karst of this kind usually has high water content and can sometimes serve as an important water source. The upper soil of the quaternary soil strata is loose. Another kind of buried karst is formed by carbonatite which is buried under hard non-carbonatites, such as metamorphic marble in Hongkong and Shenzhen. Here, the karst fractured and channels developed, forming gullies, which can be as wide as 10–20 m.

Figure 2 shows a plan view of buried karst in Guangdong Province. Buried karst is mainly distributed in north and south Guangdong Province, and the rest is in east Guangdong Province. In Zhaoqing, west Guangdong Province, the depth of buried karst is between 40 and 100 m. In the east of Guangdong Province, the buried karst is distributed among mountains. The quantity of buried karst in north Guangdong Province is huge, and it is found at high altitudes.

During the sedimentation process of limestone, primary pores are formed and tectonic movement caused joints and faults which creates conditions for rainwater to corrode the

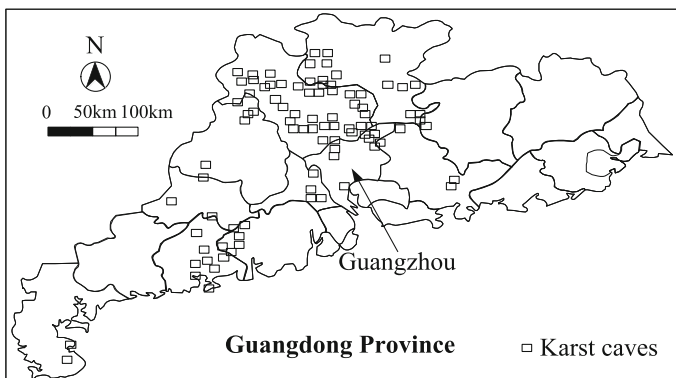


Fig. 2 Distribution of karst caves in Guangdong Province (created based on Ma 1997)

rocks. Guangdong Province, which has a subtropical monsoon climate, has year-round high temperatures and high rainfall. The abundant rainfall increases the erosion, while high temperatures accelerate biological activity, and these factors combine increasing the carbon dioxide level in the soil and result in the formation of karst caves in Guangdong Province (Yuan 1976). The shapes of the karst caves found here include sink hole, domelike hole, and hollow hole.

The karst caves are usually rich in fissure water. According to pumping tests, the permeability of these karst caves ranges from 112.2 to 135.5 m/day, and the maximum water inflow of a single karst cave is 608.8–814.7 m³/day (Yuan 1976). Karst caves are generally stable, but they collapse easily if disturbed. Most karst caves are empty or half-filled with sand or clay. The size and shape of the karst cave varies a lot.

3 Hazards of tunnelling in karst caves

Shield tunnelling is often used underground at depths of 10–30 m. When constructing in a karst region, a karst cave is likely to be encountered during the shield tunnelling process. Since the distribution of the karst caves is irregular, it is difficult to find the relationship between hazard induced by shield tunnelling and existence of the caves. If the cave has a high fissure water content, collapse is easily occurred with some disturbance. The following hazards may be encountered during tunnelling in karst caves: (1) sink holes, (2) water or stone ingress, (3) damage to constructed tunnels and the shield, and (4) long-term instability.

3.1 Sink holes

Sink holes, a geological hazard which can lead to serious casualties, may occur during tunnelling adjacent to a karst cave. Caves are stable during the long process of natural erosion. However, disturbance from tunnel construction can be disastrous. When a tunnel is constructed through caves, heavy damage could occur resulting in the collapse of the soil above into the caves. An attempt to predict this type of collapse, using probabilistic

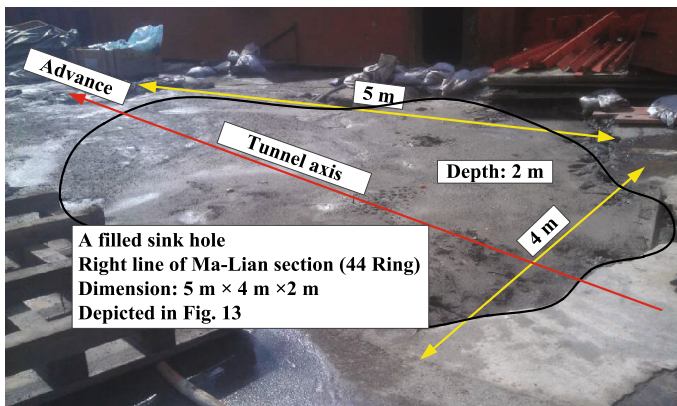


Fig. 3 A sink hole of right tunnel of Ma-Lian section due to the proximity of karst cave during tunnelling in Guangzhou

methods and susceptibility maps, has been proposed, and it is the first attempt recorded in the international literature at the assessment of future collapses in a given gypsum karst terrain (Yilmaz 2007). To prevent damage to the tunnel, the karst cave must be treated before the tunnel construction. Sink hole occurred in the Ma-Lian section of Guangzhou metro line 9 which was due to the instability of the karst cave. As shown in Fig. 3, a sink hole suddenly opened up during tunnelling. The dimensions of the sink hole were $5\text{ m} \times 4\text{ m} \times 2\text{ m}$. The reason for the sink hole opening up was that there was a karst cave above the tunnel axis and the cave had not been treated as it had not been known about. Fortunately, there was no loss of life or injuries. After that incident, all known karst caves were checked, and the same phenomenon has not occurred again.

3.2 Water or stone ingress

As karst regions have high groundwater or confined groundwater, the screw conveyor spewing and water ingress often occur during the tunnelling process. The water flow rate may reach $8\text{--}10\text{ m}^3/\text{s}$ (Lu 2010). Large stones often accompany the water ingress, which is difficult to cut-off. Depending on the presence of geological flaws, the formation of water ingress passages in a karst tunnel falls into two categories, which are water ingress tunnel with geological flaws and water ingress tunnel with no geological flaws (Li 2009). Li and Li (2014) studied the risk assessment system for water ingress in a karst tunnel using geographic information system technology to dynamically predict the water ingress risk and to develop appropriate protective measures. They found that the extremely high-risk area of water ingress accounts for 8.99 % of the total area, that with a high-risk accounts for 22.98 %, that with a medium risk accounts for 47.02 %, and that with a low-risk accounts for 21.01 %.

3.3 Damage to constructed tunnels and the shield

The constructed tunnels and the shield may be damaged and take a long time to repair in a karst region. The shield head will go down due to instability at the tunnel face when there is a large karst cave in front of the tunnel. Tunnel alignment is difficult to control. Cutter wear or cutter destruction will happen due to the sudden load when the tunnel meets the karst cave, and it is difficult to replace the cutting tool. As there is a high groundwater level in a karst cave, the synchronous grouting slurry will flow away during the tunnelling. The ground loss will be greater and will result in large ground surface settlement. All of the above factors will result in large axis deviation, schedule delay, large ground loss, soil disturbance, or even tunnel collapse.

3.4 Long-term instability

After nearly 10-year operation of metro tunnels, long-term instability of the tunnel structure is likely to occur. Shen et al. (2014) have presented the long-term deformation behaviour of metro tunnels in the soft deposits of Shanghai. The causes of this deformation, which include sublayer subsidence, post-construction settlement induced by tunnelling disturbance, disturbance from nearby construction, changes in the hydrological regime and groundwater infiltration, and the cyclic loading of the trains, would also cause long-term instability in a karst cave region in the subsequent tunnel operation. Corrosion may

generate new erosion voids or caves, which may also create new hazards. It is therefore necessary to take measures to maintain the long-term stability of the tunnel.

4 Measures for the prevention of geohazards during tunnelling

Generally, the shield tunnel line should be designed to avoid karst caves or, if they are unavoidable, to pass through areas where fewer and smaller karst caves exist. To prevent possible hazards, all of the karst caves must be treated before tunnelling. Usually, a slurry grouting method is used to deal with small karst caves. For extra-large karst caves, reinforced concrete supporting is adopted (Lu 2010). Since most of the karst caves encountered by tunnelling are small caves, this study will focus on the treatment of small karst caves within a depth of 50 m.

4.1 Construction programmes

Figure 4 shows a flow chart of karst cave treatment. First, a preliminary investigation is conducted to explore the karst caves. The detecting techniques applied may include borehole drilling, Rayleigh wave testing, CT (computed tomography), and geotechnical radar. Then, the quantity, location, and filling of the karst caves are further detected to determine whether to apply the treatment or not. If a cave treatment is necessary, the karst caves will be treated by a grouting method, for example, sleeve-valve-pipe grouting. Finally, an unconfined compressive strength (UCS) test or a standard penetration test (SPT) is conducted to check the effectiveness of the treatment. In addition, the quality of the grouting mass and core recovery can also be inspected according to the drilling samples. Figure 5 gives a schematic diagram of the karst cave treatment. The boundary of karst cave is determined before drilling the grouting hole. Then, slurry is grouted into the karst cave via the grouting hole. Figure 6 shows slurry grouting within a karst cave. A man used sleeve-valve barrel to grout slurry into the karst cave.

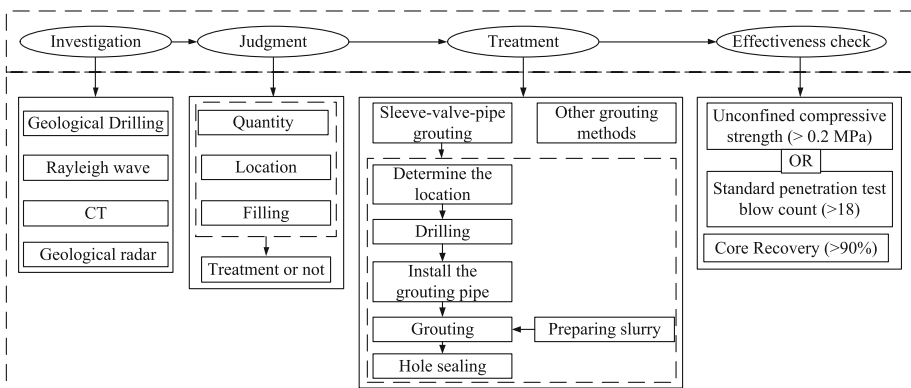


Fig. 4 Flow chart of karst cave treatment

Fig. 5 Schematic diagram of the karst cave treatment

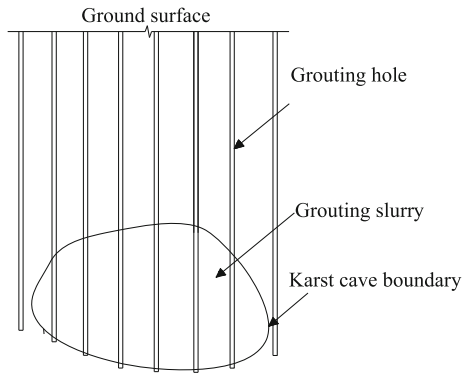
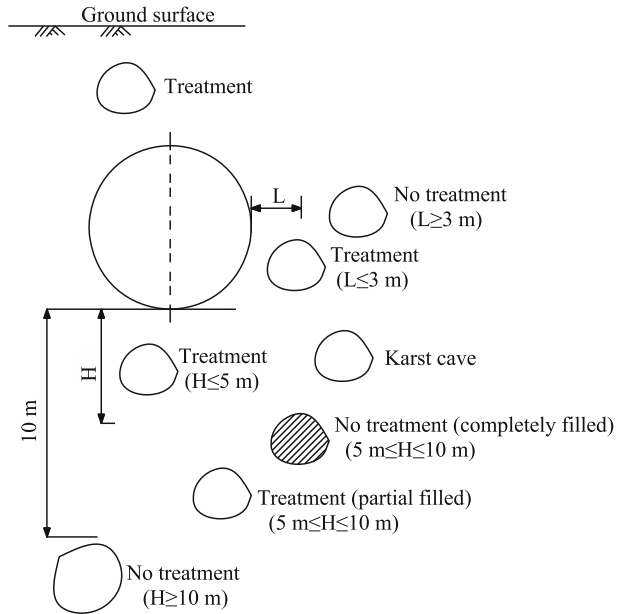


Fig. 6 Slurry grouting into the karst cave

4.2 Treatment criteria

Figure 7 shows the treatment criteria of the karst caves around a tunnel (GMDRI 2010). A karst cave must be treated if it is above the tunnel axis. In the horizontal direction, if L (the distance from the tunnel in the horizontal direction) is less than 3 m, the karst cave must be treated. However, in the vertical direction, if H (the distance below the tunnel in the vertical direction) is less than 5 m and the karst cave is not filled up, the karst cave must be treated. If H is between 5 and 10 m and the karst cave is completely filled up, then no treatment is necessary. If the karst cave is partially filled and H is between 5 and 10 m, the karst cave must be treated. If H is greater than 10 m, the karst does not have to be treated.

Fig. 7 Treatment criteria of karst caves around tunnel



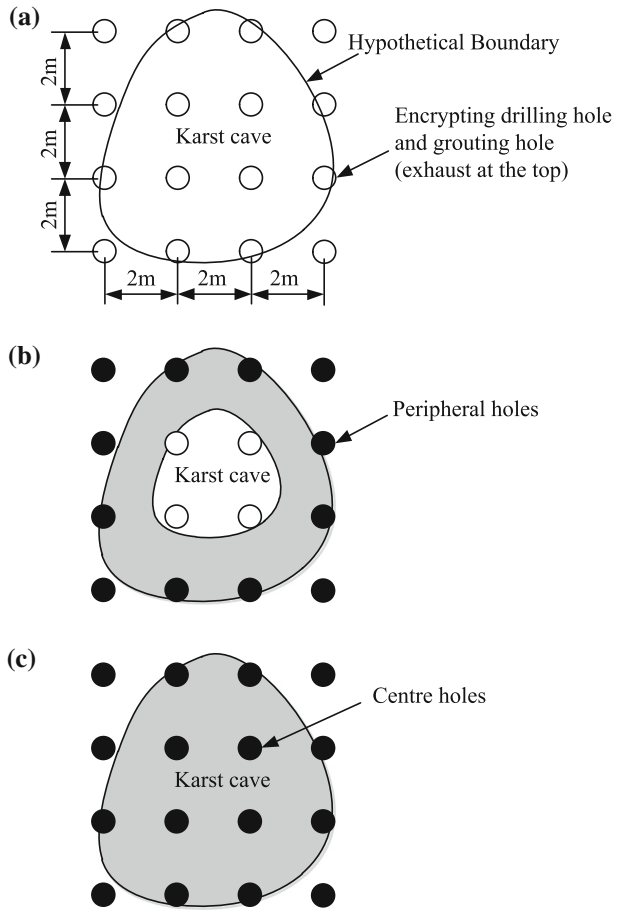
4.3 Grouting steps

Figure 8a shows the layout of the grouting holes. The grouting process for each hole is shown in Fig. 9. The grouting holes are drilled in a rectangular pattern at 2 m spacing, to a depth of 0.2–0.3 m below the bottom of the karst cave. The peripheral holes are grouted first (Fig. 8b), and then, the centre holes are grouted (Fig. 8c). After drilling the grouting hole, the grouting pipe is inserted down to the bottom of the hole and grouting begins (Fig. 9a). The initial grouting pressure is 0.3–0.4 MPa, and the grouting rate is 30–70 L/min. When the grouting pressure exceeds 0.5 MPa, the grouting pipe is lifted up by 0.4 m and grouting and then continues. This process is repeated until the grouting pipe reaches the top of the karst cave (Fig. 9b). Grouting should be stopped when the grouting pressure stays at 1.2 MPa for 10 min (Fig. 9c). The procedure is then carried out at the next grouting hole and repeated until all of the holes are grouted and the karst cave is completely filled with grouting material.

4.4 Grouting material

Two kinds of slurry, single slurry and binary slurry, are used to fill the karst caves. The single slurry, which is made of water, cement, and sand with a mass ratio of 0.8:1:1, is used to fill the central holes (Fig. 8). In order to shorten the time of flow, sodium silicate, which can fasten the gelling of cement, is added into the single slurry to make binary slurry. The binary slurry is used for the grouting of the peripheral holes (Fig. 8). The gelling time can be acquired via laboratory mixing ratio test, and the suggested mass ratio of water, cement, sand, and sodium silicate of binary slurry is (0.8–1):1:1:(0.08–0.2). The cement is ordinary Portland cement and the Baume degree of the sodium silicate is 38–43 Bé. In practice, soil and water from the cave and sodium silicate are used to conduct the mixing ratio test

Fig. 8 Layout of the grouting holes

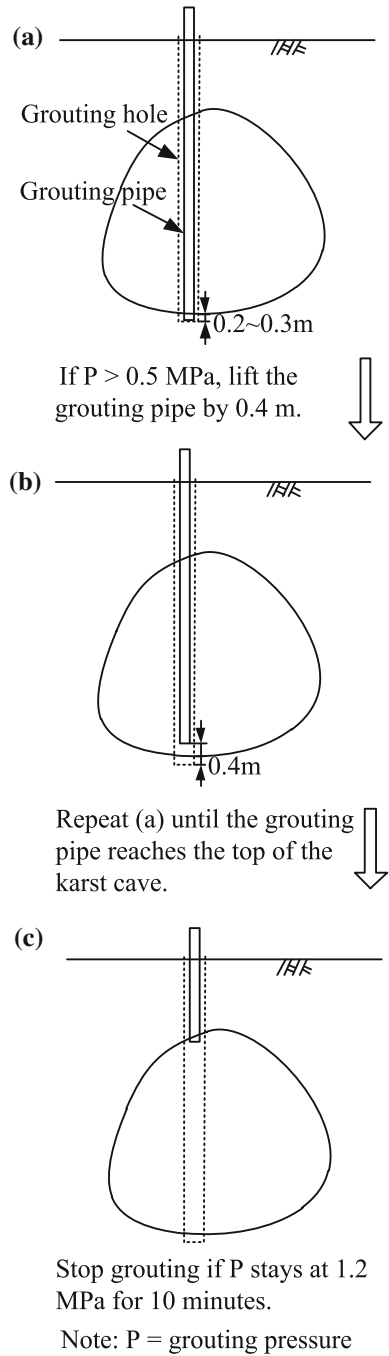


before the treatment of the karst cave. Since the soil type and water from each cave are different, content of sodium silicate should be changed.

4.5 Effectiveness check

The following parameters were documented from an inspection of the karst cave treatment: unconfined compressive strength (UCS), standard penetration test (SPT), and core recovery (CR). UCS or SPT is used to check the strength of the grouting mass, and the CR is used to check the integrity of the grouting mass. Every karst cave must be inspected. One per cent of the total holes, and no less than 3 holes, should be spot-checked. The drilling–coring method should be adopted to obtain the test sample. Twenty-eight days after the karst cave treatment, UCS tests and standard penetration tests should be conducted on the core samples. The required unconfined compressive strength after 28 days should be greater than 0.2 MPa, the modified blow count based on a SPT should be greater than 10, and the core recovery (CR) should be greater than 90 %. The grouting mass achieved at the same depth of a karst cave of the test sample should be solidified cement–soil.

Fig. 9 Grouting process for one hole



5 Case study of karst cave treatment during tunnelling in Guangdong

5.1 Description of construction site

Figure 10a shows a map of the Guangzhou metro tunnel system. Figure 10b shows the plan view of metro line 9. The test site is a tunnel section of the Maanshan Park Station to Liantangan Station route (Ma-Lian section) on metro line 9, the construction of which involved the use of two earth pressure balance shield machines and began on 16 November 2013 and was completed on 1 July 2014. The metro tunnel axis is located at a depth of 9.8 m. The lining of the tunnel has an outer diameter of 6 m and an inner diameter of 5.4 m.

Figure 11 plots the geotechnical profiles and soil properties of the test site. The subsoil profile consisted of backfill (from 1.1 to 5 m deep), sand (from 1.7 to 20.4 m deep), silty clay (from 5 to 25.5 m deep), highly weathered limestone (from 11.3 to 22.0 m deep), residual soil of limestone (13.4 to 27.8 m deep), limestone (from 14.5 to 23.5 m deep), and slight weathered limestone (from 15.2 to 40.8 m deep). The natural water content of the soil in this test site ranges from 20 % (in the residual soil of limestone layer) to 46.2 % (in the sand layer). The hydraulic conductivity of the sand layer is about 5–15 m/day. The UCS of the limestone is about 44.7 MPa. The soil in the tunnel zone mainly consists of a highly weathered limestone layer, a sand layer, and a silty clay layer.

The tunnelling progress of passing the monitoring zone of right tunnel and left tunnel from ring No. 243 (R243) to ring No. 432 (R432) is shown in Fig. 12. The right tunnel was constructed prior to that for the left tunnel. As can be seen, the advance rate of the right tunnel (5.9 rings per day) was slightly higher than that of the left tunnel (5.4 rings per day).

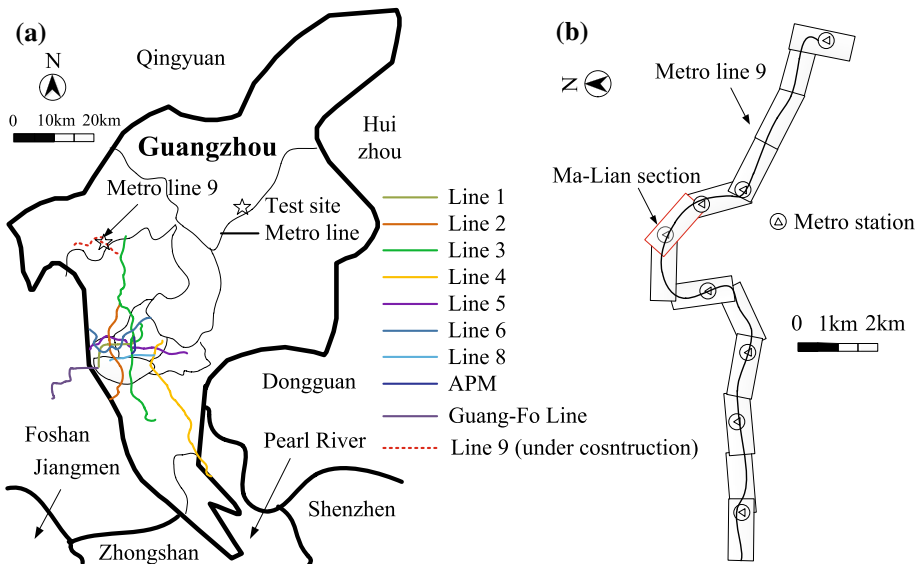


Fig. 10 Map of metro system in Guangzhou and location of test site

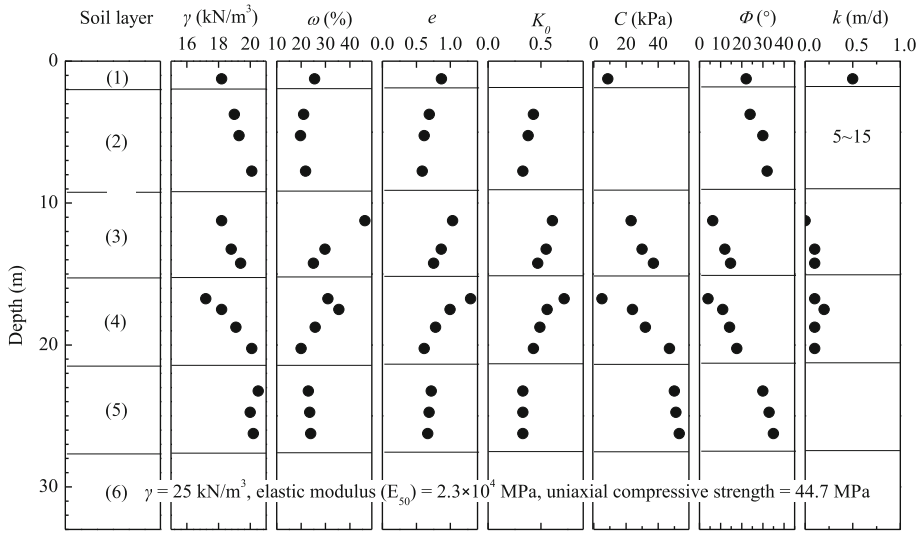


Fig. 11 Geotechnical profiles and soil properties of the subsoil

5.2 Treatment of karst caves before tunnelling

5.2.1 Investigation

A geological drilling method was used to investigate the karst caves in the Ma-Lian section. Three holes were drilled to obtain the soil samples. These were located in the middle or on either side of the tunnel section with 3-m spacing. After analysis of the drilled soil samples, 98 karst caves were found along the tunnel. Figure 13 shows a plan view of the 98 karst caves in Ma-Lian section, and the vertical diameter of the caves is listed in Table 1. As can be seen, 13.3 % of the karst caves were higher than 5 m. Figure 14 shows the treatment results of the 98 karst caves. According to the treatment criteria (Fig. 7), 50 karst caves needed to be treated (Fig. 14).

5.2.2 Treatment

This investigation focuses on a selected monitoring zone of the Ma-Lian section which has 43 karst caves, which are densely distributed along its length. The length of this tunnel section is about 285 m from ring number 243 (R243) to ring number 432 (R432). The plan view of these 43 karst caves is also shown in Fig. 14. As shown in Fig. 14, the hollow circles stand for karst caves which need no treatment, and the solid black circles stand for karst caves which need treatment. Figure 15 shows a sectional view of the selected monitoring zone. A–A is the longitudinal section of left line. B–B is the longitudinal section between left line and right line. C–C is the longitudinal section of the right line. The karst caves are all below the tunnel zone. The depth of the karst cave top and the vertical diameters of the 25 karst caves requiring treatment are listed in Table 2. Single slurry and binary slurry were used to fill these 25 karst caves.

Fig. 12 Tunnelling progress curve when passing the monitoring zone: **a** right tunnel and **b** left tunnel

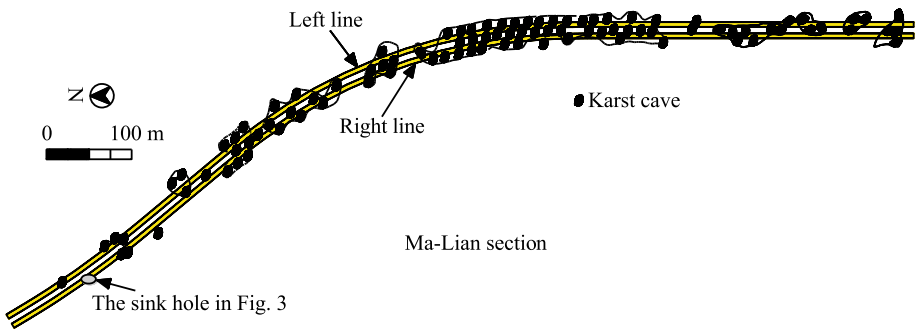
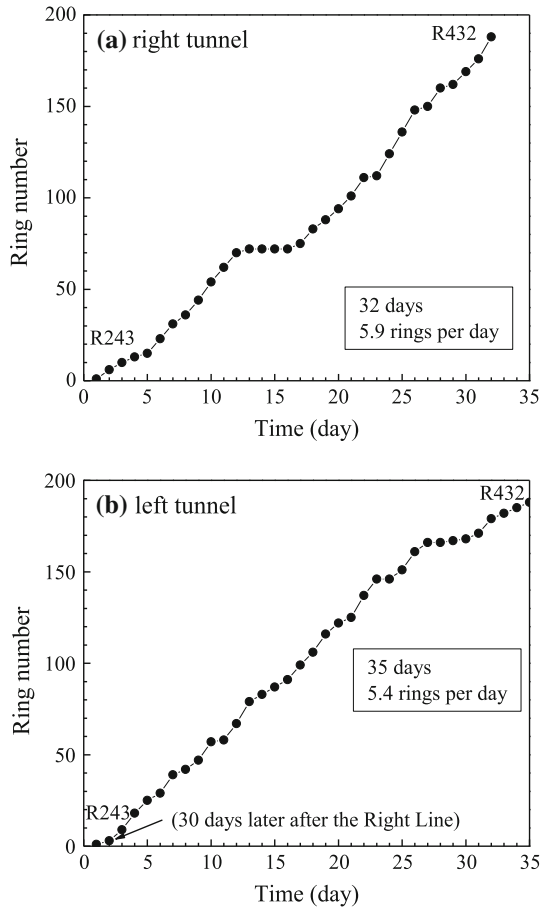


Fig. 13 Distribution of karst caves in Ma-Lian section

Table 1 Vertical diameter distribution of the 98 detected karst caves

Vertical diameter (D , m)	Percentage (%)
$D < 1$ m	24.5
$1 \text{ m} < D < 3$ m	48
$3 \text{ m} < D < 5$ m	14.3
$D > 5$ m	13.3

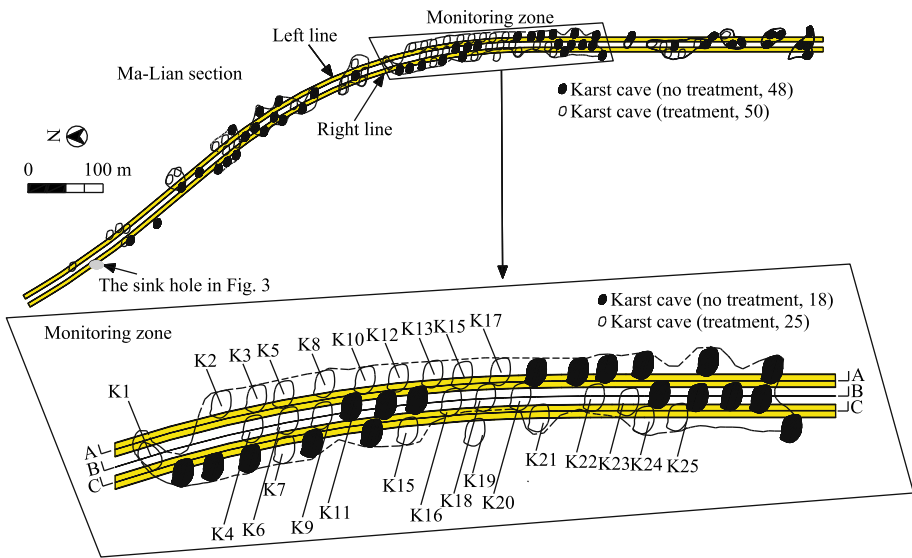


Fig. 14 Treatment of karst caves and a selected monitoring zone of Ma-Lian section

5.2.3 Effectiveness inspection

Unconfined compressive strength tests and standard penetration tests were conducted on borehole samples of K1–K25 after 28 days. Figure 16 shows the modified SPT and UCS for the 25 karst caves. As shown in Fig. 16, the modified SPT values are all above 10. The minimum and maximum values of the UCS are about 1.1 and 1.5 MPa, respectively, and the UCS values are all above 0.2 MPa. These test results indicate that construction within these 25 karst caves can satisfy the bearing requirement. A soil sample from one of the karst caves was obtained by drilling 28 days after grouting. The core recovery (CR) value is also shown in Fig. 16, and the values are all greater than 90 %. The borehole sample obtained from each drilling location at the same depth of the karst cave consisted of solidified cement–soil. It can be concluded that the quality of the treatment of the 25 karst caves was good, which created safe conditions for the subsequent tunnelling excavation.

Figure 17 shows the borehole samples of K13 and K20. As can be seen from the K13 sample, there was solidified cement–soil at the depth of the karst cave. The colour of the solidified cement–soil was tan. The solidified cement–soil was a mass made up of a combination of sand and cement slurry. Additionally, there was grey solidified cement–soil at the depth of the karst cave for the K20, which was a combination of silty clay and cemented slurry.

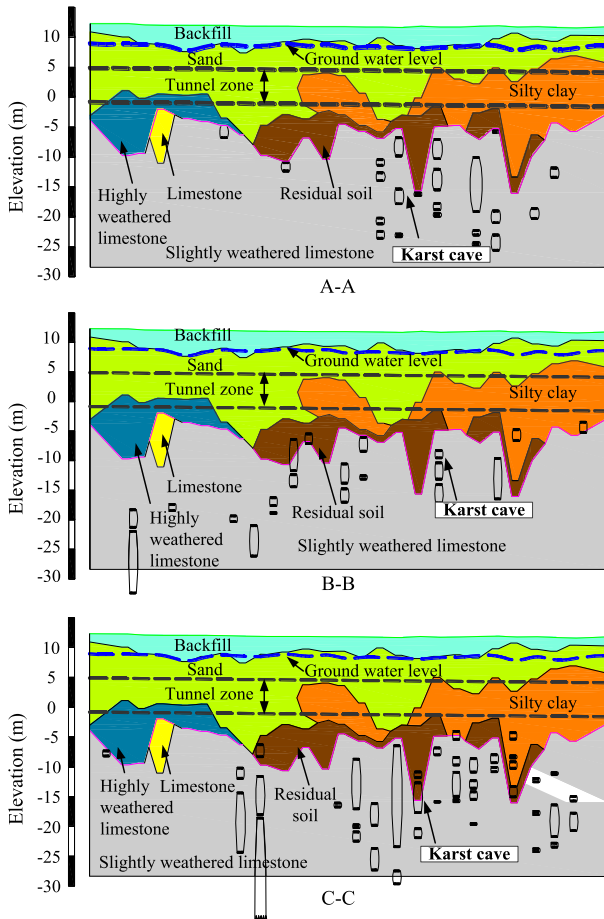


Fig. 15 Geological section views of tunnel zones

5.3 Environmental impacts of tunnelling

5.3.1 Monitoring instrumentation

Figure 18 shows a plan view of the monitoring instrumentation. Building settlement and ground surface settlement were monitored to study the environmental effects due to tunnelling after karst cave treatment. Four level gauges, near to the two buildings, were used to measure the ground surface settlement at R314 and R358 (Fig. 18). Gauges labelled S1 and S3, and S2 and S4 were located along the axis of the left tunnel and the right tunnel, respectively. The monitoring frequency for the instruments was once a day during the initial tunnelling phase. When the TBM reached beyond 30 m from the monitoring point, the monitoring frequency was increased to three times a day.

Table 2 General profile of the 25 karst caves

Karst cave number	Depth of karst cave top (m)	Vertical diameter (m)	Single slurry (m ³)	Binary slurry (m ³)
K1	0.39	1.2	263.37	–
K2	11.04	4.5	4.30	–
K3	3.57	0.6	6.20	–
K4	3.29	0.7	187.91	–
K5	2.88	1	525.07	–
K6	5.2	0.7	358.22	–
K7	3.1	0.5	305.6	–
K8	6.26	0.86	352.99	–
K9	7.25	1.38	180.59	–
K10	9.86	1.79	272.11	–
K11	3.14	0.64	374.07	450.92
K12	9.37	2.56	213.05	216.35
K13	8.09	1.31	92.72	–
K14	6.68	0.82	351.82	78.83
K15	5.46	0.63	182.83	–
K16	6.98	0.9	317.78	–
K17	6.31	1.05	121.68	–
K18	3.38	0.65	408.84	–
K19	6.54	1.15	306.58	150.29
K20	8.84	0.84	389.64	291.20
K21	9.67	0.71	365.81	–
K22	1.36	0.74	241.90	–
K23	5.48	0.67	2.60	–
K24	2.88	0.62	320.81	–
K25	3.28	0.64	444.61	81.85

5.3.2 Ground surface settlement and building settlement

Figure 19a shows the ground surface settlement of S1 due to the tunnelling excavation of the right tunnel. Before the TBM approached S1, there was no settlement. After the TBM passed S1, the ground surface settlement increased rapidly. Then, the settlement tended towards a stable value of approximately 41 mm when the TBM was 30 m from S1. Figure 19b–d shows the ground surface settlement of S2, S3, and S4 due to the tunnelling excavation. The patterns of settlement of S1, S2, and S3 are similar. The maximum ground settlement of S2 and S3 were 30.1 and 29.6 mm. There was about 3 mm heave before the TBM approached S3 and S4. As shown in Fig. 19d, there was 15 mm settlement when the TBM was 52 m from S4. However, the maximum ground settlement of S4 was 29.4 mm.

Figure 19a–d shows surface heaving in front of tunnel face. During tunnelling in karst region, pressure at the cutter face should be a little bit higher than the lateral earth pressure to avoid collapse of cutter face of shield. Therefore, before the shield reaches the measuring point, there is a little bit heave, and after that, there will be a settlement. As shown in Fig. 19a–d, the first stepwise is the result of the gap between shield machine and tunnel lining and these settlement formed with shield tail leaving lining at the measuring point,

Fig. 16 SPT values of karst caves, UCS values of drilling samples, and core recovery (K1–K25)

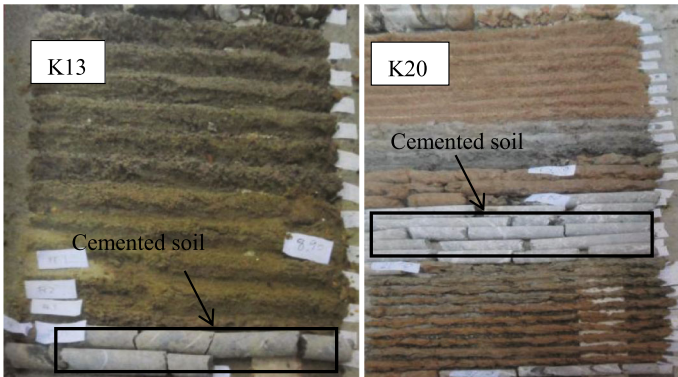
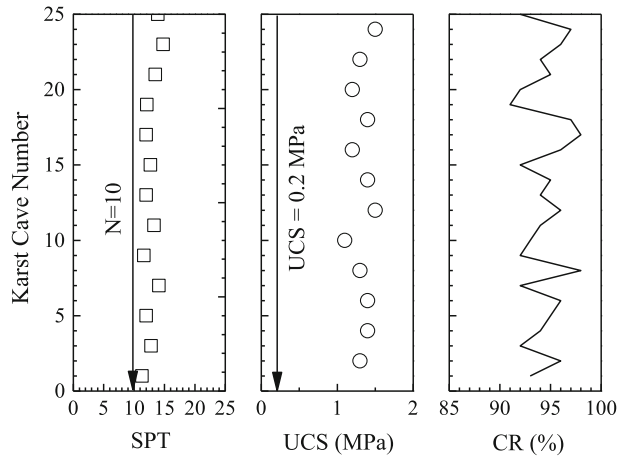


Fig. 17 Geological drilling samples of *K13* and *K20* after 28 days

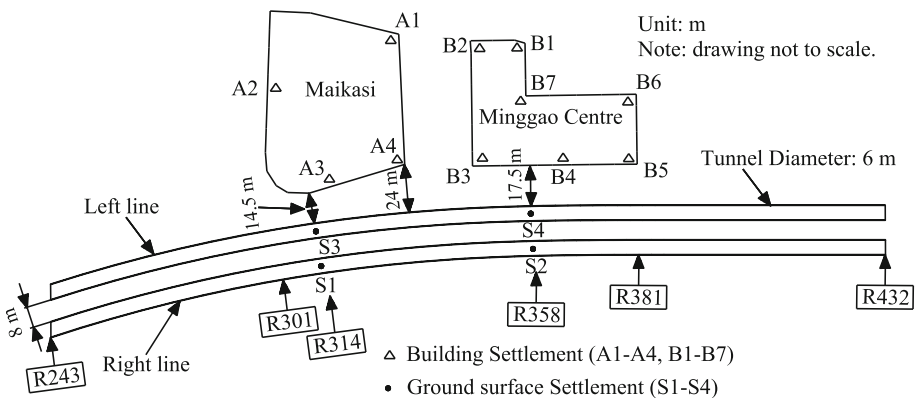
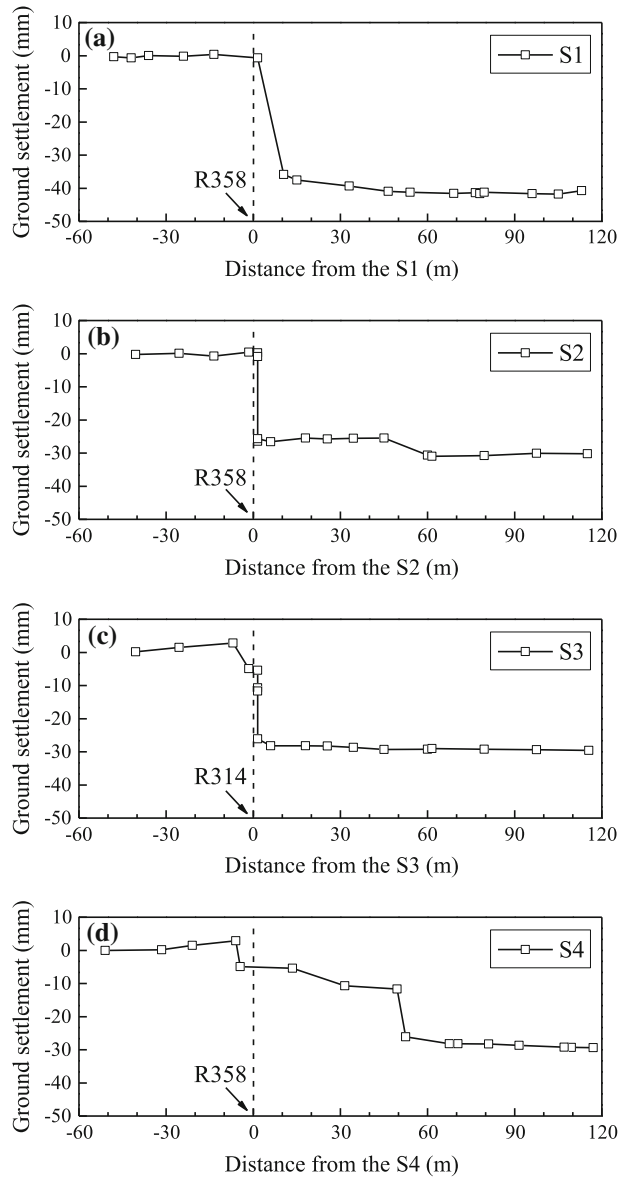


Fig. 18 Plan view of building settlement gauges and ground surface settlement gauges

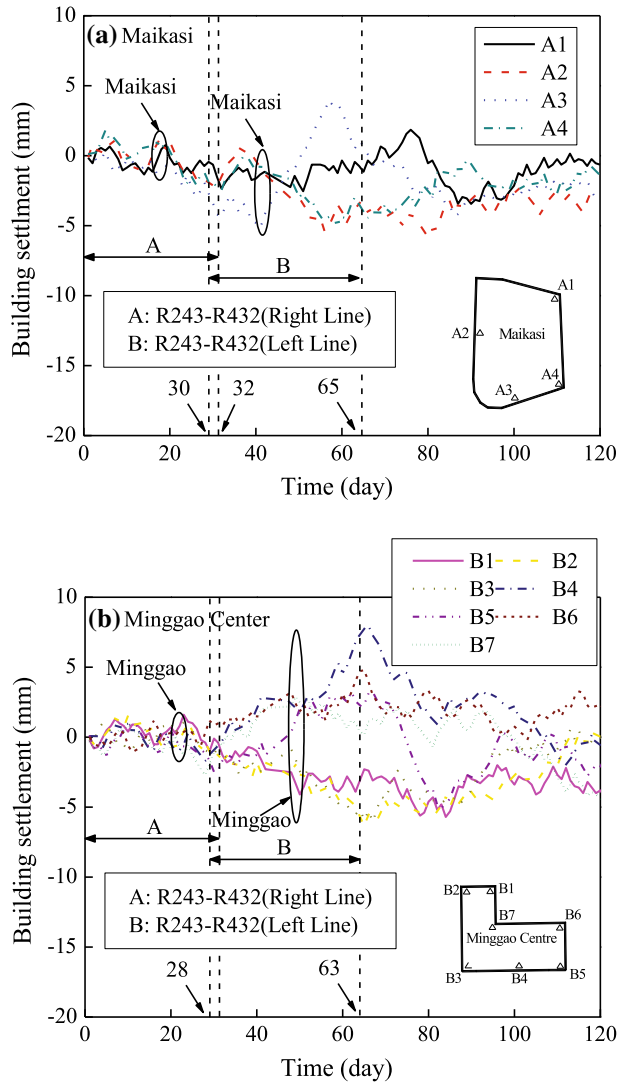
Fig. 19 Ground surface settlement of S1, S2, S3, and S4



which is common in most shield tunnelling. And the second stepwise in Fig. 19d may be caused by the collapse of a small karst cave over the tunnel.

Figure 20a, b shows the vertical displacement of Maikasi and Minggao Center due to the tunnelling excavation. As shown in Fig. 20a, the building settlement increased during the tunnelling excavation of the right tunnel and fluctuated during the tunnelling of the left tunnel. After 80 days, the building settlement tended to be stable. The range of the building settlement was within ± 5 mm. As shown in Fig. 20b, the settlement changed within 2 mm

Fig. 20 Settlement of buildings: **a** Maikasi and **b** Minggao Centre



during the tunnelling of the right tunnel. However, a heave developed at B4–B7 during the tunnelling of the left tunnel, and the maximum heave was 8 mm. This was followed by about 5 mm settlement after 63 days. After the left tunnel passed the Minggao Centre, the displacement of B1–B7 tended to be stable and remained within 5 mm.

Even though there was 30–40 mm ground surface settlement and ± 10 mm building settlement, the TBM passed through the selected monitoring zone successfully, apart from a sink hole developing as a result of a sink hole (mentioned above). No other accidents happened during the tunnelling excavation of the metro lines. The important practical conclusion from the field test is the verification of the applicability of this treatment process in karst regions.

6 Conclusions

The following conclusions can be drawn.

- a. Karst, formed by carbonatite, is widely distributed in China, and buried karst is widely distributed in Guangdong Province. The subtropical monsoon climate of Guangdong Province leads to increased erosion and the formation of buried karst. Buried karst (karst caves), which are under the ground up to a depth of 50 m, could affect engineering construction work. Karst caves are often empty or half-filled with sand or clay and can be rich in fissure water.
- b. Karst caves can remain stable if there is no disturbance. However, many hazards will appear when tunnelling in karst regions, such as sink holes, water or stone ingress, damage to constructed tunnels and the shield, and long-term instability.
- c. To avoid the potential risks, a treatment technique, which involves filling the karst caves, is proposed in this study. After geotechnical investigation of the tunnelling zone, the quantity, location, and condition of the karst caves are assessed to determine whether or not the treatment should be applied. The karst caves are then treated by grouting with single slurry or binary slurry, for example, by sleeve-valve-pipe grouting. Finally, the effectiveness of the karst cave treatment is inspected through UCS, SPT, and CR after 28 days.
- d. The construction quality and environmental impacts of the treatment technique are examined through a case study. The modified SPT values of the karst caves were all greater than 10, and the UCS values of the borehole samples were all greater than 0.2 MPa. It can be concluded that the treatment of these 25 karst caves can satisfy engineering requirements.
- e. The ground surface settlement and building settlement are all within the allowable values. Based on this case, it can be concluded that the karst cave treatment method can satisfy the engineering requirements and provide a database to guide future engineering practice in karst regions.

Acknowledgments The research work described herein was funded by the National Nature Science Foundation of China (NSFC) (Grant Nos. 41372283 and 41472252) and National Basic Research Programme of China (973 Programme: 2015CB057800). These financial supports are gratefully acknowledged.

References

- Fargnoli V, Boldini D, Amorosi A (2013) TBM tunnelling-induced settlements in coarse-grained soils: the case of the new Milan underground line 5. *Tunn Undergr Space Technol* 38:336–347. doi:[10.1016/j.tust.2013.07.015](https://doi.org/10.1016/j.tust.2013.07.015)
- Guangzhou Metro Design & Research Institute Co., Ltd (GMDRI) (2010) General technical requirement of karst treatment in Guangzhou Metro Line 9 (Trial) (in Chinese)
- Gui L (2008) Engineering technique for shield tunnel in karst region of Guangzhou Metro Line 5. *J Guilin Univ Technol* 28(3):324–329 (in Chinese)
- Ju SJ, Zhu WB (2007) Study on geological investigation methods for shield tunneling in mixed ground. *Tunn Constr* 27(6):10–14 (in Chinese)
- Li LP (2009) Study on catastrophe evolution mechanism of karst water Inrush, PhD Thesis. Shandong University, Jinan, Shandong (in Chinese)
- Li X, Li Y (2014) Research on risk assessment system for water inrush in the karst tunnel construction based on GIS: case study on the diversion tunnel groups of the Jinping II hydropower station. *Tunn Undergr Space Technol* 40:182–191. doi:[10.1016/j.tust.2013.10.005](https://doi.org/10.1016/j.tust.2013.10.005)

- Li SC, Zhou ZQ, Li LP, Xu ZH, Zhang QQ, Shi SS (2013) Risk assessment of water inrush in karst tunnels based on attribute synthetic evaluation system. *Tunn Undergr Space Technol* 38:50–58. doi:[10.1016/j.tust.2013.05.001](https://doi.org/10.1016/j.tust.2013.05.001)
- Liao SM, Peng FL, Shen SL (2008) Analysis of shearing effect on tunnel induced by load transfer along longitudinal direction. *Tunn Undergr Space Technol* 23(4):421–430. doi:[10.1016/j.tust.2007.07.001](https://doi.org/10.1016/j.tust.2007.07.001)
- Liao SM, Liu JH, Wang RL, Li ZM (2009) Shield tunneling and environment protection in Shanghai soft ground. *Tunn Undergr Space Technol* 24(4):454–465. doi:[10.1016/j.tust.2008.12.005](https://doi.org/10.1016/j.tust.2008.12.005)
- Lu YR (2010) China karst. Higher Education Press, Beijing (in chinese)
- Ma LF (1997) The topographic map of the People's Republic of China. China Atlas Press, Beijing (in Chinese)
- Ma L, Xu YS, Shen SL, Sun WJ (2014) Evaluation of the hydraulic conductivity of aquifers with piles. *Hydrogeol J* 22(2):371–382. doi:[10.1007/s10040-013-1068-y](https://doi.org/10.1007/s10040-013-1068-y)
- Shen SL, Xu YS (2011) Numerical evaluation of land subsidence induced by groundwater pumping in Shanghai. *Can Geotech J* 48(9):1378–1392. doi:[10.1139/T11-049](https://doi.org/10.1139/T11-049)
- Shen SL, Xu YS, Hong ZS (2006) Estimation of land subsidence based on groundwater flow model. *Mar Georesour Geotechnol* 24(2):149–167. doi:[10.1080/10641190600704848](https://doi.org/10.1080/10641190600704848)
- Shen SL, Horpibulsuk S, Liao SM, Peng FL (2009) Analysis of the behavior of DOT tunnel lining caused by rolling correction operation. *Tunn Undergr Space Technol* 24(1):84–90. doi:[10.1016/j.tust.2008.05.003](https://doi.org/10.1016/j.tust.2008.05.003)
- Shen SL, Du YJ, Luo CY (2010) Evaluation of the effect of double-o-tunnel rolling-correction via apply one-side block loading. *Can Geotech J* 47(10):1060–1070. doi:[10.1139/T10-013](https://doi.org/10.1139/T10-013)
- Shen SL, Wang ZF, Yang J, Ho EC (2013a) Generalized approach for prediction of jet grout column diameter. *J Geotech Geoenviron Eng ASCE* 139(12):2060–2069. doi:[10.1061/\(ASCE\)GT.1943-5606.0000932](https://doi.org/10.1061/(ASCE)GT.1943-5606.0000932)
- Shen SL, Wang ZF, Sun WJ, Wang LB, Horpibulsuk S (2013b) A field trial of horizontal jet grouting using the composite-pipe method in the soft deposits of Shanghai. *Tunn Undergr Space Technol* 35:142–151. doi:[10.1016/j.tust.2013.01.003](https://doi.org/10.1016/j.tust.2013.01.003)
- Shen SL, Wang ZF, Horpibulsuk S, Kim YH (2013c) Jet-grouting with a newly developed technology: the twin-jet method. *Eng Geol* 152(1):87–95. doi:[10.1016/j.enggeo.2012.10.018](https://doi.org/10.1016/j.enggeo.2012.10.018)
- Shen SL, Wu HN, Cui YJ, Yin ZY (2014) Long-term settlement behavior of the metro tunnel in Shanghai. *Tunn Undergr Space Technol* 40:309–323. doi:[10.1016/j.tust.2013.10.013](https://doi.org/10.1016/j.tust.2013.10.013)
- Shin HS, Kim CY, Kim KY, Bae GJ, Hong SW (2006) A new strategy for monitoring of adjacent structures to tunnel construction in urban area. *Tunn Undergr Space Technol* 21:461–462. doi:[10.1016/j.tust.2005.12.099](https://doi.org/10.1016/j.tust.2005.12.099)
- Standing J, Selemetas D (2013) Greenfield ground response to EPBM tunnelling in London Clay. *Géotechnique* 63(12):989–1007. doi:[10.1680/geot.12.P.154](https://doi.org/10.1680/geot.12.P.154)
- Tan Y, Wang DL (2013a) Characteristics of a large-scale deep foundation pit excavated by central-island technique in Shanghai soft clay. I: bottom-up construction of the central cylindrical shaft. *ASCE J Geotech Geoenviron Eng* 139(11):1875–1893. doi:[10.1061/\(ASCE\)CF.1943-5509.0000521](https://doi.org/10.1061/(ASCE)CF.1943-5509.0000521)
- Tan Y, Wang DL (2013b) Characteristics of a large-scale deep foundation pit excavated by central-island technique in Shanghai soft clay. II: top-down construction of the peripheral rectangular pit. *ASCE J Geotech Geoenviron Eng* 139(11):1894–1910. doi:[10.1061/\(ASCE\)CF.1943-5509.0000535](https://doi.org/10.1061/(ASCE)CF.1943-5509.0000535)
- Tóth Á, Gong Q, Zhao J (2013) Case studies of TBM tunnelling performance in rock–soil interface mixed ground. *Tunn Undergr Space Technol* 38:140–150. doi:[10.1016/j.tust.2013.06.001](https://doi.org/10.1016/j.tust.2013.06.001)
- Wu HN, Huang RQ, Sun WJ, Shen SL, Xu YS, Liu YB, Du SJ (2014) Leaking behaviour of shield tunnels under the Huangpu river of Shanghai with induced hazards. *Nat Hazards* 70(2):1115–1132. doi:[10.1007/s11069-013-0863-z](https://doi.org/10.1007/s11069-013-0863-z)
- Xu YS, Shen SL, Cai ZY, Zhou GY (2008) The state of land subsidence and prediction activities due to groundwater withdrawal in China. *Nat Hazards* 45(1):123–135. doi:[10.1061/40867\(199\)5](https://doi.org/10.1061/40867(199)5)
- Xu YS, Ma L, Shen SL, Sun WJ (2012a) Evaluation of land subsidence by considering underground structures that penetrate the aquifers of Shanghai, China. *Hydrogeol J* 20(8):1623–1634. doi:[10.1007/s11069-012-0220-7](https://doi.org/10.1007/s11069-012-0220-7)
- Xu YS, Ma L, Du YJ, Shen SL (2012b) Analysis on urbanization induced land subsidence in Shanghai. *Nat Hazards* 63(2):1255–1267. doi:[10.1007/s11069-012-0220-7](https://doi.org/10.1007/s11069-012-0220-7)
- Xu YS, Shen SL, Du YJ, Chai JC, Horpibulsuk S (2013a) Modelling the cutoff behavior of underground structure in multi-aquifer-aquitard groundwater system. *Nat Hazards* 66(2):731–748. doi:[10.1007/s11069-013-0576-3](https://doi.org/10.1007/s11069-013-0576-3)
- Xu YS, Huang RQ, Han J, Shen SL (2013b) Evaluation of allowable withdrawn volume of groundwater based on observed data. *Nat Hazards* 67(2):513–522. doi:[10.1061/\(ASCE\)GT.1943-5606.0000527](https://doi.org/10.1061/(ASCE)GT.1943-5606.0000527)
- Yang YS, Wu H, Xu JF, Yang XQ (2007) Construction of shield tunnel in karst strata. *J Railw Eng Soc* 7:56–60 (in Chinese)

- Yilmaz I (2007) GIS based susceptibility mapping of karst depression in gypsum: a case study from Sivas basin (Turkey). *Eng Geol* 90(1–2):89–103. doi:[10.1016/j.enggeo.2006.12.004](https://doi.org/10.1016/j.enggeo.2006.12.004)
- Yuan DX (1976) Karst in China. Shanghai People's Publishing House, Shanghai (in Chinese)
- Zhang Q, Tian S, Mo Y, Dong X, Hao S (1993) An expert system for prediction of karst disaster in excavation of tunnels or underground structures through a carbonate rock area. *Tunn Undergr Space Technol* 8(3):373–378. doi:[10.1016/0886-7798\(93\)90021-M](https://doi.org/10.1016/0886-7798(93)90021-M)
- Zhao J, Gong QM, Eisensten Z (2007) Tunnelling through a frequently changing and mixed ground: a case history in Singapore. *Tunn Undergr Space Technol* 22(4):388–400. doi:[10.1016/j.tust.2006.10.002](https://doi.org/10.1016/j.tust.2006.10.002)